RESEARCH ARTICLE

Journal of **Applied Toxicology** WILEY

Farnesoid X receptor contributes to oleanolic acid-induced cholestatic liver injury in mice

Hong Feng[1,2] 🟢 | Yan Hu[2] | Shaoyu Zhou[2] | Yuanfu Lu[2] 🟢

[1]People's Hospital of Zunyi City Bo Zhou District, Zunyi, China

[2]Key Laboratory of Basic Pharmacology of the Ministry of Education and Joint International Research Laboratory of Ethnomedicine of the Ministry of Education, Zunyi Medical University, Zunyi, China

Correspondence

Shaoyu Zhou and Yuanfu Lu, Key Laboratory of Basic Pharmacology of the Ministry of Education and Joint International Research Laboratory of Ethnomedicine of the Ministry of Education, Zunyi Medical University, Zunyi, Guizhou 563003, China.
Email: luyuanfu2000@163.com; szhou20@163.com

Abstract

Farnesoid X receptor (FXR) is a nuclear receptor involved in the metabolism of bile acid. However, the molecular signaling of FXR in bile acid homeostasis in cholestatic drug-induced liver injury remains unclear. Oleanolic acid (OA), a natural triterpenoid, has been reported to produce evident cholestatic liver injury in mice after a long-term use. The present study aimed to investigate the role of FXR in OA-induced cholestatic liver injury in mice using C57BL/6J (WT) mice and FXR knockout (FXR$^{-/-}$) mice. The results showed that a significant alleviation in OA-induced cholestatic liver injury was observed in FXR$^{-/-}$ mice as evidenced by decreases in serum alanine aminotransferase, aspartate aminotransferase, and alkaline phosphatase as well as reduced hepatocyte necrosis. UPLC-MS analysis of bile acids revealed that the contents of bile acids decreased significantly in liver and serum, while increased in the bile in FXR$^{-/-}$ mice compared with in WT mice. In addition, the mRNA expressions of hepatic transporter *Bsep*, bile acid synthesis enzymes *Bacs* and *Baat*, and bile acids detoxifying enzymes *Cyp3a11*, *Cyp2b10*, *Ephx1*, *Ugt1a1*, and *Ugt2b5* were increased in liver tissues of FXR$^{-/-}$ mice treated with OA. Furthermore, the expression of membrane protein BSEP was significantly higher in livers of FXR$^{-/-}$ mice compared with WT mice treated with OA. These results demonstrate that knockout of FXR may alleviate OA-induced cholestatic liver injury in mice by decreasing accumulation of bile acids both in the liver and serum, increasing the export of bile acids via the bile, and by upregulation of bile acids detoxification enzymes.

KEYWORDS
bile salt export pump (BSEP), cholestasis, FXR, liver injury, oleanolic acid

1 | INTRODUCTION

Drug-induced cholestatic liver injury (DIC) is caused by damaged bile acid homeostasis and is the primary pattern of drug-induced liver injury (Hoofnagle & Björnsson, 2019). DIC may further develop into serious consequences such as liver fibrosis, liver cirrhosis, liver cancer, and liver failure and has become the key factor of drug

withdrawal (Li & Apte, 2015). A portion of Traditional Chinese Medicine (TCM) has been considered hepatotoxic based on modern medicine theory, although they are still widely prescribed in the clinic and have been used to treat various diseases for over 2000 years (Liu et al., 2020). The development of modern medicine and a wider application of Chinese herbal medicine have led to an increased incidence of TCM-associated liver toxicity, and especially

DIC has increasingly been identified (Liu et al., 2020; Oh et al., 2015). Oleanolic acid (OA) is a natural triterpenoid that is widely used as a complementary and alternative medicine in China and other countries (Liu et al., 2018). Several studies have indicated that OA treatment may lead to liver toxicity if given in small doses for an extended period or in a large dose over a short time (Liu et al., 2018). Previously, we found that OA induced cholestatic liver injury in Kunming mice administered with OA at a dose of 225 mg/kg once daily for 10 consecutive days (Lu et al., 2013) or in C57BL/6J male mice treated with OA at 457–685.5 mg/kg once a day for four consecutive days (Feng et al., 2020). Nonetheless, the mechanisms underlying OA-induced cholestatic liver injury have yet to be defined.

Bile acids are synthesized in the liver using cholesterol as the raw material through two routes: "classical" and "alternative" (Wei et al., 2018). The classical pathway is regulated by cholesterol 7a-hydroxylase (*Cyp7a1*), cholesterol 8b-hydroxylase (*Cyp8b1*), and cholesterol 27a-hydroxylase (*Cyp27a1*) and produces cholic acid (CA). The alternative pathway is regulated by *Cyp27a1* and cholesterol 7b-hydroxylase (*Cyp7b1*), which produces chenodeoxycholic acid (CDCA). The free bile acids are conjugated to glycine (G) and taurine (T) through bile acid-CoA synthetase (*Bacs*) and bile acid-CoA amino acid N-acyltransferase (*Baat*). Many transporters are involved in the active transport of bile acids across the canalicular membrane to form bile, including bile salt export pump (*Bsep*), multidrug resistance-associated protein 2 (*Mrp2*) and multidrug resistance protein 2 (*Mdr2*). Among these transporters, *Bsep* plays a major role in efflux pathways (Song et al., 2015). Most of the bile acids are finally reabsorbed back to the liver through the Na+-taurocholate cotransport protein (*Ntcp*), and the organic anion transporter (*Oatp*), namely, bile acid enterohepatic circulation. During circulation, increased production of bile acids, excessive intake, and decreased excretion can contribute to cholestatic liver injury (Feng & Lu, 2020). Previously, we found that OA-induced liver injury occurred in mice when treated with OA at the dose of 90–135 mg/kg daily for 5 days mice developed liver injury with increased levels of serum ALT, AKP, and TBA. Serum unconjugated and conjugated bile acids in the OA-treated animals were increased, but the expression levels of *Fxr*, *Bsep*, *Ntcp*, *Oatp1b2*, *Cyp7b1*, *Cyp8b1*, and *Cyp3a11* were decreased (Liu et al., 2013), suggesting that OA-induced liver injury was associated with bile acid homeostasis.

FXR plays a pivotal role in regulation of bile acid homeostasis. It is mainly expressed in hepatocytes, regulates hepatic bile acid biosynthesis and transport proteins, and participates in the formation, secretion, transport, uptake, and detoxification of bile acids (Shin & Wang, 2019). Activation of FXR can lead to suppression of bile acid synthesis enzymes such as *Cyp7a1* and *Cyp8b1* via small heterodimer chaperone (*Shp*) or fibroblast growth factor 15/19 (*FGF15/19*) pathways (Li & Chiang, 2013) and the hepatic influx transporters (*Ntcp* and *Oatp*) (Feng & Lu, 2020). FXR also upregulates hepatic efflux transporters *Bsep*, *Mrp2*, and *Mdr2* and liver detoxification enzymes UDP-glucuronyltransferase (*Ugt1a1* and *Ugt2b5*), sulfotransferases (*Sult2a1*), hepatic microsomal epoxide hydrolase (*Ephx1*), and liver

drug metabolism enzymes (*Cyp3a11* and *Cyp2b10*), thereby mitigating intrahepatic bile acid overload and alleviating cholestatic liver injury. In contrast, studies have demonstrated that after inhibiting FXR or FXR gene knockout, the bile acid synthesis enzymes (*Cyp7a1* and *Cyp27a1*) and uptake transporters (*Ntcp* and *Oatp*) were increased, while the bile acid efflux transporters (*Bsep* and *Mdr2*) and liver detoxification enzymes (*Ugt1a1*, *Cyp3a11*, and *Cyp2b10*) were decreased, resulting in bile acid overload and decreased bile acid detoxification ability, leading to increased toxicity (Cariello, Piccinin, Garcia-Irigoyen, Sabbà, & Moschetta, 2018; Yuan & Li, 2016). In addition, it has been demonstrated that knockout of FXR can ameliorate the increased liver injury in obstructive cholestasis by increasing the expression of the transporters *Bsep* and *Mdr4*, and by lowering serum and hepatic bile acid concentrations, suggesting a potential clinical role for FXR antagonists in the treatment of obstructive cholestatic liver disorders (Stedman et al., 2006). Based on these results, we propose that there may exist a beneficial effect of the downregulation of FXR in the homeostasis of bile acids in a pathological setting of OA-induced cholestatic liver injury.

Accordingly, in the present study, we aimed to investigate the regulatory role of FXR in OA-induced cholestasis using C57BL/6J mice and FXR gene knockout mice.

2 | MATERIALS AND METHODS

2.1 | Materials

OA (purity > 99%) was obtained from Sigma-Aldrich company (St. Louis, USA). HPLC grade acetonitrile was purchased from Thermo Fisher Scientific (CA, USA), and ammonium acetate was purchased from Sigma-Aldrich (St. Louis, USA). The following 48 bile acid standards were purchased from ZZBIO LTD (Shanghai, China), they were listed as follows: glycoursodeoxycholic acid, GUDCA; glycholic acid, GCA; taurohyodeoxycholic acid, THDCA; tauroursodeoxycholic acid, TUDCA; taurocholic acid, TCA; cholic acid, CA; ursodeocholic acid, UDCA; ursocholic acid, UCA; hyodeocholic acid, HDCA; glycohyodeoxycholic acid, GCDCA; taurodeoxycholic acid TDCA; taurochenodeoxycholic acid, TCDCA; glycodeoxycholic acid, GDCA; chenodeocholic acid, CDCA; lithocholic acid, LCA; deoxycholic acid, DCA; taurolithocholic acid, TLCA; glycodehydrocholic acid, GDHCA; dehydrocholic acid, DHCA; 3β-cholic acid, 3β-CA; tauro β-muricholic acid, T β-MCA; α-muricholic acid, α-MCA; 3β-ursodeoxycholic acid, β-UDCA; 7-ketodeoxycholic acid, 7-keto DCA; hyocholic acid, HCA; taurolithocholic acid 3 sulfate, TLCA-3S; 3β-hyodeocholic acid, β-HDCA; chenodeocholic acid-3-β-D-glucuronide, CDCA-3G; 6-ketolithocholic acid, 6-Keto LCA; lithocholic acid 3 sulfate, LCA-3S; 6,7-diketolithocholic acid, 6,7-Diketo LCA; 7-ketolithocholic acid, 7-Keto LCA; 12-ketolithocholic acid, 12-Keto LCA; 7,12-diketolithocholic acid, 7,12-Diketo LCA; taurohyocholic acid, THCA; Nor Cholic acid, NorCA; glycohyodeoxycholic acid 3 sulfate, GCDCA-3S; β-muricholic acid, β-MCA; glyhyocholic acid, GHCA; tauro α-muricholic acid, T-αMCA; lithocholic acid 3 sulfate, LCA-3S;

allocholic acid, ACA; chenodeoxycholic acid-24-β-D-glucuronide, CDCA-24G; 23-nordeoxycholic acid, NorDCA; apocholic acid, ApoCA; isodeoxycholic acid, IsoDCA; isolithocholic acid, ILCA; and allolithocholic acid, AlloLCA.

2.2 | Animal experiments

Male C57BL/6J (wild-type, WT) mice were purchased from SPF Biotechnology Co. Ltd (Beijing, China), and matched $FXR^{-/-}$ mice were provided by Dr. Lili Ji, Institute of Chinese Medicine, Shanghai University of Traditional Chinese Medicine. Mice were raised in a controlled room under a 12-h light–dark cycle and were fed normal chow and were given free access to water. After a standard rodent chow for 7 days, mice were divided into three groups randomly ($n = 8$), including control group (Control, 10 ml/kg corn oil), OA low dose group (OA-L, 457 mg/kg), and OA high dose group (OA-H, 685.5 mg/kg). The doses used were based on a previous study (Feng et al., 2020; Lu et al., 2013); corn oil and OA were administered intragastrically once per day for 4 days, respectively. Body weights were controlled daily; at the end of the last dose administration, mice were treated with an intraperitoneal injection of pentobarbital anesthesia (60 mg/kg) (Shi et al., 2019). Mice were sterilized abdominally; following an approximately 2 cm longitudinal longitudinal transrectal incision, the abdomen was exposed to reveal the veins. Serum, liver, and gallbladder samples were collected. Blood was incubated at room temperature for 30 min, and serum fractions were obtained from blood by centrifugation for 15 min (1600 g, 4°C) for biochemical reagent detection and bile acid profile analysis. After liver samples were weighed, they were divided into two parts: one part was immediately frozen in liquid nitrogen and then stored in −80°C for further research, and another part was soaked in 4% neutral formalin for histological evaluation. Gallbladders also were immediately frozen in liquid nitrogen and then stored in −80°C until use.

2.3 | Ethics statement

All procedures involving animals were in accordance with the National Institutes of Health guide for the care and use of Laboratory animals (NIH Publications No. 8023, revised 1978) and approved by Institutional Animal Use and Care Committee of Zunyi Medical University.

2.4 | Serum chemistry

Serum samples were analyzed using standard enzymatic assays using commercial kits for alanine aminotransferase (ALT), aspartate aminotransferase (AST), alkaline phosphatase (ALP), and total bile acid (TBA) in accordance with the manufacturer's protocols (Jiang-Cheng Biological, China).

2.5 | Histopathology

Liver tissues were fixed in 4% neutral buffered formalin solution for 24 h and then embedded in paraffin, and 3.5-μm-thick sections were obtained by cutting with a Leica RM2245 Biosystems microtome (Wetzlar, Germany). The slices were successively washed, dehydrated, and stained with hematoxylin and eosin (HE) for pathological examination (Olympus BX43, Tokyo, Japan). According to the area of liver tissue cell necrosis, hepatic necrosis was graded on a scale of 0 to 4+, in which score 0, represented no necrosis; score 1+, represented necrosis of 5–30% of hepatocytes; score 2+, represented necrosis of 30–50% of hepatocytes; score 3+, represented necrosis of 50–70% of hepatocytes; and score 4+, represented necrosis over 70% of hepatocytes (Oz et al., 2003). Each slide was evaluated blinded by two of our investigators (Hong Feng and Yan Hu) using light microscope; five fields were observed randomly at 200 times for each slice.

2.6 | Bile acids profiling analysis using UPLC-MS

2.6.1 | Sample preparation

Samples were collected as described previously (Huang et al., 2019; Lu, Du, Qin, Ma, et al., 2018). For liver samples, approximately 100 mg frozen liver tissues were accurately weighed and homogenized in 2 volumes of ddH_2O (200 μl for 100 mg). The mixtures were centrifuged for 15 min (13,500 g, 4°C), and 250 μl supernatants were transferred to clean tubes. Next, supernatants were treated with 500 μl acetonitrile, swirled for 30 s, centrifuged for 15 min (13,500 g, 4°C), and then precipitated proteins and other particulates were removed. Finally, 600 μl supernatants were transferred to clean tubes; the samples were evaporated to dryness with nitrogen and redissolved in 100 μl 50% methanol solution (methanol: $dddH_2O = 50:50$, v/v). After centrifuging for 15 min (13,500 g, 4°C), the supernatants were used for further quantification. For serum samples, 100 μl serum samples were spiked with 200 μl acetonitrile, swirled for 30 s, and then centrifuged for 15 min (13,500 g, 4°C). A volume of 180 μl supernatants was transferred to clean tubes. Samples were treated as indicated above for processing of liver samples. For bile samples, 1 μl volume of bile samples was spiked with 200 μl acetonitrile, swirled for 30 s, and centrifuged 15 min (13,500 g, 4°C). The subsequent steps were treated as indicated above for processing serum samples.

2.6.2 | Relative quantification of bile acids

Based on our previous studies (Huang, 2019; Huang et al., 2019; Lu, Du, Qin, Wu, et al., 2018), the samples were collected for analysis of the bile acid profiling by using Ultra Performance Liquid Chromatography (UPLC)-Q Exactive Orbitrap-mass spectrometry (MS) and Xcalibur workstation (Thermo, USA). Sample analysis was carried out under negative electrospray (ESI) mode. The scan mode was Full Scan/dd-MS2. The detailed parameters were as follows: spray voltage of

3.2 kV, the capillary temperature of 350°C, the sheath of 35 arbitrary units, auxiliary gas flow rates of 15 arbitrary units. The mass scanning range was m/z 100–1000. The chromatographic separation was achieved on a Thermo Hypersil Gold C_{18} column (2.1 × 150 mm, 1.9 μm), column temperature 40°C. The mobile phase consisted of 20% acetonitrile with 10 mM ammonium acetate (A) and 80% acetonitrile with 10 mM ammonium acetate (B), flow rate: 0.3 ml/min, injection volume: 2 μl. The initial composition of the mobile phase was 5% B, which was changed to 14% B in 6 min and then changed to 25% B in 6.3 min, hereafter changed to 50% B, maintaining the ratio for 10 min. It was then changed to 5% B, and after 3 min, it was changed to 100% B and held for 0.5 min, then changed to 5% B for 4 min. Peak areas were used for comparison and statistical analysis. Bile acids were recognized and relatively quantified through the comparison with bile acid standards, including retention time, molecular weight, and mass spectra (Huang et al., 2019).

2.7 | RNA extraction and real-time polymerase chain reaction analysis

Total RNA of liver tissues was extracted using the TRIzol reagent (Takara Bio Inc., Japan) according to the manufacturer's instructions. RNA quality was determined by the 260/280 ratio (>1.8), and cDNA was synthesized using the PrimeScript RT Reagent Kit (TakaRa,

China). Relative gene expression was determined using the quantitative PCR (qPCR) method and the CFX Connect (Bio-Rod, USA) with the iQ™ SYBR® GREEN qPCR kit (Bio-Rod, USA). The reaction was carried on in a final reaction volume of 15 μl as recommended by the manufacturer, using the PCR primers listed in Table 1. The qRT-PCR thermal program was run as follows: 10 s at 95°C and 45 s at 60°C for the reverse transcription and 39 cycles and then 5 s at 55–95°C for melt curve. The cycle threshold ($\Delta\Delta Ct$) values were used to calculate relative mRNA expression, which were normalized with GAPDH, and expressed as relative transcript levels, setting WT mice control group as 100%.

2.8 | Western blotting analysis

Liver membrane proteins were extracted using the ProteinExt™ Membrane Protein Extraction Kit (Tran, China). The protein content was quantified by the BCA Protein Assay Kit (Beyotime, China) and prepared for gel loading with 5× sample buffer (Zoman, China). The samples (16 μg) were separated by 8–10% SDS-polyacrylamide gel and transferred onto a polyvinylidene fluoride (PVDF) membrane. The nonspecific binding sites of the membrane were blocked with 5% nonfat dry milk before probing with Anti-Bsep antibody (1:1000, Thermo, USA) and GAPDH (1:10,000, Proteintech, China) at 4°C overnight. Next, the membrane was incubated with the HRP-conjugated

TABLE 1 Primer sequences

Genes	Gen bank number	Forward (5′-3′)	Reverse (5′-3′)
Fxr	XM_030244963	CGGAACAGAAACCTTGTTTCG	TTGCCACATAAATATTCATTGAGATT
Cyp7a1	NM_007824	ACACCATTCCTGCAACCTTC	GCTGTCCGGATATTCAAGGA
Cyp27a1	XM_006495607	CTGCGTCAGGCTTTGAAACA	TCGTTTAAGGCATCCGTGTAGA
Bsep	XM_006499670	ACAGCACTACAGCTCATTCAGAG	TCCATGCTCAAAGCCAATGATCA
Cyp8b1	NM_010012	GCCTTCAAGTATGATCGGTTCCT	GATCTTCTTGCCCGACTTGTAGA
Ntcp	NM_001361972	ATCTGACCAGCATTGAGGCTC	CCGTCGTAGATTCCTTGCTGT
Ostα	NM_145932	TACAAGAACACCCTTTGCCC	CGAGGAATCCAGAGACCAAA
Ostβ	NM_178933	GTATTTTCGTGCAGAAGATGCG	TTTCTGTTTGCCAGGATGCTC
Shp	NM_011850	CAGCGCTGCCTGGAGTC	AGGATCGTGCCCTTCAGGTA
Cyp7b1	XM_006535384	CTTTTGGACTCGGAACAAGC	CGGGGTGCTGAATACCTAAA
Oatp1b2	XM_036166208	TCAGGACACCAAGACTGCTG	TTGCTTGGATGCTGAGTTTG
Mdr2	XM_036164874	CATTTCCAAGTCTGGGAGGA	AACACAGCCAACCTTGGAAC
Mrp2	XM_006526625	GCACTGTAGGCTCTGGGAAG	CATTTCCAAGTCTGGGAGGA
Ugt1a1	XM_030255057	ATCATGCCCAACATGGTTTT	TGCATCAAACAGCTCCTGAC
Ugt2b5	NM_009467	TTGGAGTTTCCTCACCCAAC	TTGCGTTGGCTTTTTCTTCT
Sult2a1	NM_001111296	TCGGCTGGAATCCTAAGAGA	GGCACAGTTTGGATCCACTT
Cyp2b10	NM_009999	CTCTCCTTGTGGGCTTCTTG	CCACACAGCATAACCACAGG
Cyp3a11	NM_007818	CAGCTTGGTGCTCCTCTACC	CTCTGGGTCTGTGACAGCAA
Ephx1	NM_001312918	TTCCTGGCTATGGCTTCTCAGAGG	TCGCCGCCTTGAATGTAGAACTTC
Bacs	NM_009512	TCTATGGCCTAAAGTTCAGGCG	CTTGCCGCTCTAAAGCATCC
Baat	NM_007519	GTCCTCCCTTGGATAGCCTGA	CCGGATGCGGCTTTCCTTA
Gapdh	NM_008084	GGTGAAGGTCGGTGAAG	CTCGCTCCTGGAAGATGGTG

Affinipure Goat Anti-Rabbit IgG (1:5000, Proteintech, China) secondary antibody at room temperature for 40 min. All antibodies were dissolved in TBST (with 1% BSA). The signals were detected using an electrochemiluminescence kit (7 Sea Biotech, China) with a chemiluminescence detection system (Bio-Rad, USA), and the density of the immunoreactive bands was then analyzed.

3 | STATISTICAL ANALYSIS

All experimental data were expressed as mean ± standard error of the mean (SEM). and were evaluated using SPSS 18.0. Data were assessed using one-way analysis of variance (ANOVA) and followed by the LSD (equal variance assumed) or Dunnett' T3 (equal variance not assumed) test. The graphs were generated using GraphPad Prism version 7 (GraphPad Software). A P value of <0.05 was considered statistically significant.

4 | RESULTS

4.1 | Cholestatic liver injury is reduced in FXR$^{-/-}$ mice after OA administration

The changes of body weight, liver index and serum biochemical indicators were evaluated following continuous OA administration for 4 days to determine the liver injury. As shown in Figure 1A, after OA was administered for 4 days, the body weight of WT mice in the OA-H group decreased significantly compared with the control group. There was no significant difference in the body weight of FXR$^{-/-}$ mice between the control group and the OA-H group. Compared with the control group, the gallbladder weight and liver index of the WT mice increased markedly in the high dose OA-treated (Figure 1B,C). These results showed that liver injury occurred in the WT mice, while significantly less injury was found in the FXR$^{-/-}$ mice when treated with high dose of OA.

The levels of serum ALT, AST, ALP, and TBA were increased in both the OA-L and OA-H groups compared with the control group among WT mice (Figure 2), while the increases in the OA-H group were more profound, and particularly, the ALP level of the OA-H group was 2.37 times the upper level of normal (ULN), suggesting that cholestatic liver injury occurred in the WT mice of the OA-H group (Trauner et al., 2019). In the FXR$^{-/-}$ mice, the serum ALT, AST, and ALP levels also increased in the OA-H group after OA administration compared with the control group of FXR$^{-/-}$ mice, but the ALP level of the OA-H group was 1.45 times the ULN, which suggested that cholestatic liver injury had not occurred in FXR$^{-/-}$ mice (Trauner et al., 2019). Notably, in the OA-H group mice, all these serum biochemical indicators of FXR$^{-/-}$ mice were significantly lower than those of WT mice. More importantly, the serum TBA level was not elevated in the FXR$^{-/-}$ mice while a dramatic increase was observed in WT mice (Figure 2D). The liver histopathology was used to further evaluate the liver injuries (Figure 3), which was agreed with the serum
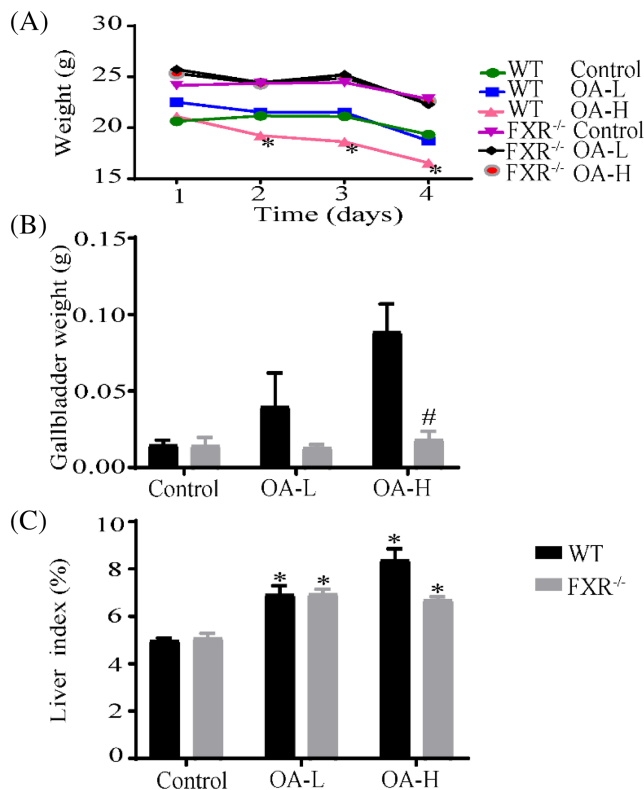
FIGURE 1 Changes of body weight and liver index after OA continuous administration for 4 days. Measurements were conducted at 24 h after the last dose (OA-L: oleanolic acid low dose group; OA-H: oleanolic acid high dose group). Data are presented as the mean ± SEM ($n = 5$–8). *$P < 0.05$, as compared with the control group without OA treatment; #$P < 0.05$, comparison between WT mice and FXR$^{-/-}$ mice under the same dose of OA treatment

biochemical results. In WT mice, no lesions appeared in the control group, but necrosis of hepatocytes (black arrows) was observed in both OA-L and OA-H groups, and the extent of hepatocyte necrosis was dose-dependent, suggesting that the hepatocyte necrosis occurred in WT mice was caused by OA rather than spontaneous lesion in mice (Kawashita et al., 2019). While the hepatocyte necrosis did not occur in FXR$^{-/-}$ mice, some swelling hepatocytes (black arrows) were observed in the liver tissues of FXR$^{-/-}$ mice. These findings demonstrated that knockdown of FXR$^{-/-}$ attenuated OA-induced cholestatic liver injury in mice.

4.2 | Bile acids levels are lower in FXR$^{-/-}$ mice than in wild-type mice following OA administration

Cholestatic liver injury is mainly caused by the accumulation of bile acids in the bile acid pool especially in the liver. Individual bile acids differ in their relative cytotoxicity, and changes to the composition of the bile acid pool can modulate hepatic injury. Therefore, we quantified the individual bile acid concentrations both in WT mice and FXR$^{-/-}$ mice following OA administration. We found that OA treatment induced changes in the profile of bile acids, and conjugated bile
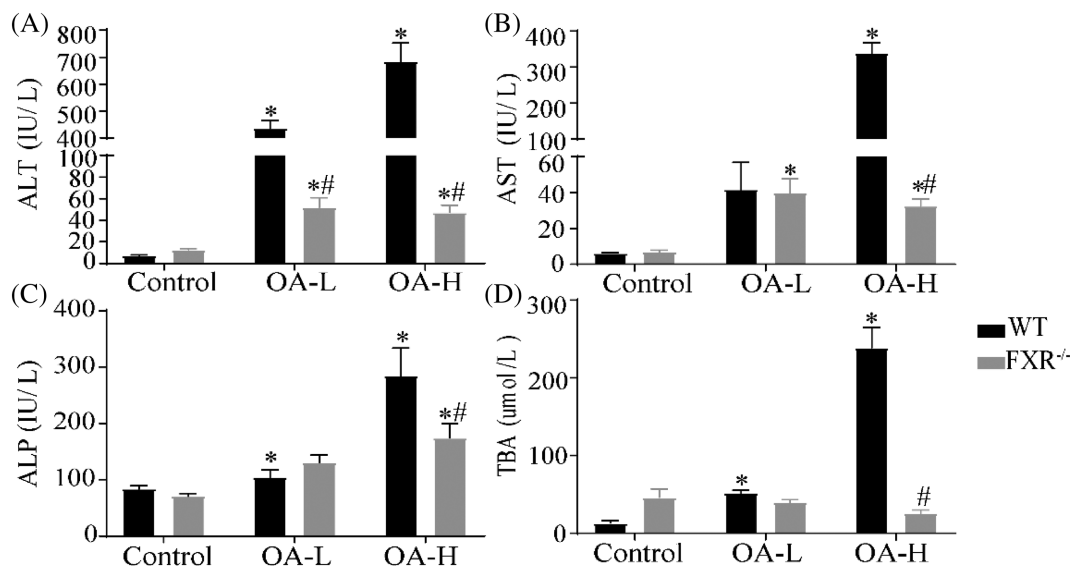
FIGURE 2 Serum biochemical analysis after OA continuous administration for 4 days. Measurements were conducted at 24 h after the last dose (OA-L: oleanolic acid low dose group; OA-H: oleanolic acid high dose group). Data are presented as the mean ± SEM (n = 5–8). *P < 0.05, as compared with the control group without OA treatment; #P < 0.05, comparison between WT mice and FXR$^{-/-}$ mice under the same dose of OA treatment
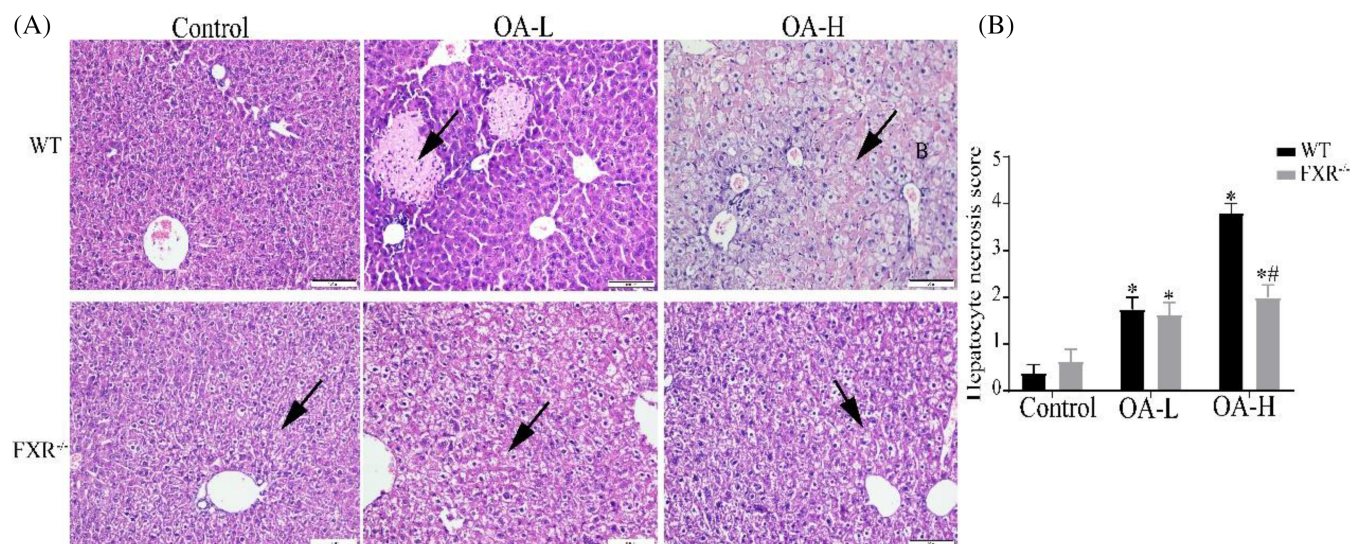
FIGURE 3 Hematoxylin–eosin staining of liver tissues after OA continuous administration for 4 days. Tissues were collected at 24 h after the last dose (OA-L: oleanolic acid low dose group; OA-H: oleanolic acid high dose group). Representative images (A) were shown in ×200 magnification, arrows represented swelling of liver cells and necrosis of liver cells, and hepatic necrosis was graded on a scale (B). Data are presented as the mean ± SEM (n = 5–8). *P < 0.05, as compared with the control group without OA treatment; #P < 0.05, comparison between WT mice and FXR$^{-/-}$ mice under the same dose of OA treatment

acids were the leader in the liver, serum, and bile, with relatively low content of free bile acids (no shown) at 24 h after the last dose following OA continuous administration for 4 days. As illustrated in Figure 4, in WT mice, compared with the control group, TCA, GCA, TDCA, GDCA, TCDCA, and T-α/βMCA were increased in the liver following OA-H, suggesting that increased liver bile acids levels contributed to OA-induced cholestatic liver injury. In FXR$^{-/-}$ mice, compared with control group, TCA, GCA, TDCA, GDCA, TUDCA, TLCA, THDCA,

TCDCA, and T-α/βMCA were increased in the OA-H group. However, the levels of TCA, GCA, TDCA, TUDCA, TLCA, THDCA, TCDCA, and T-αMCA in the liver after OA-H treatment were all significantly higher in the FXR$^{-/-}$ mice than those in the WT mice. It has been reported that liver TBA levels increased in the early stages of α-naphthyl isothiocyanate (ANIT) administration, but showed only a small range of fluctuation after ANIT-induced cholestatic hepatotoxicity (Yang et al., 2017). In this regard, we questioned that OA-induced
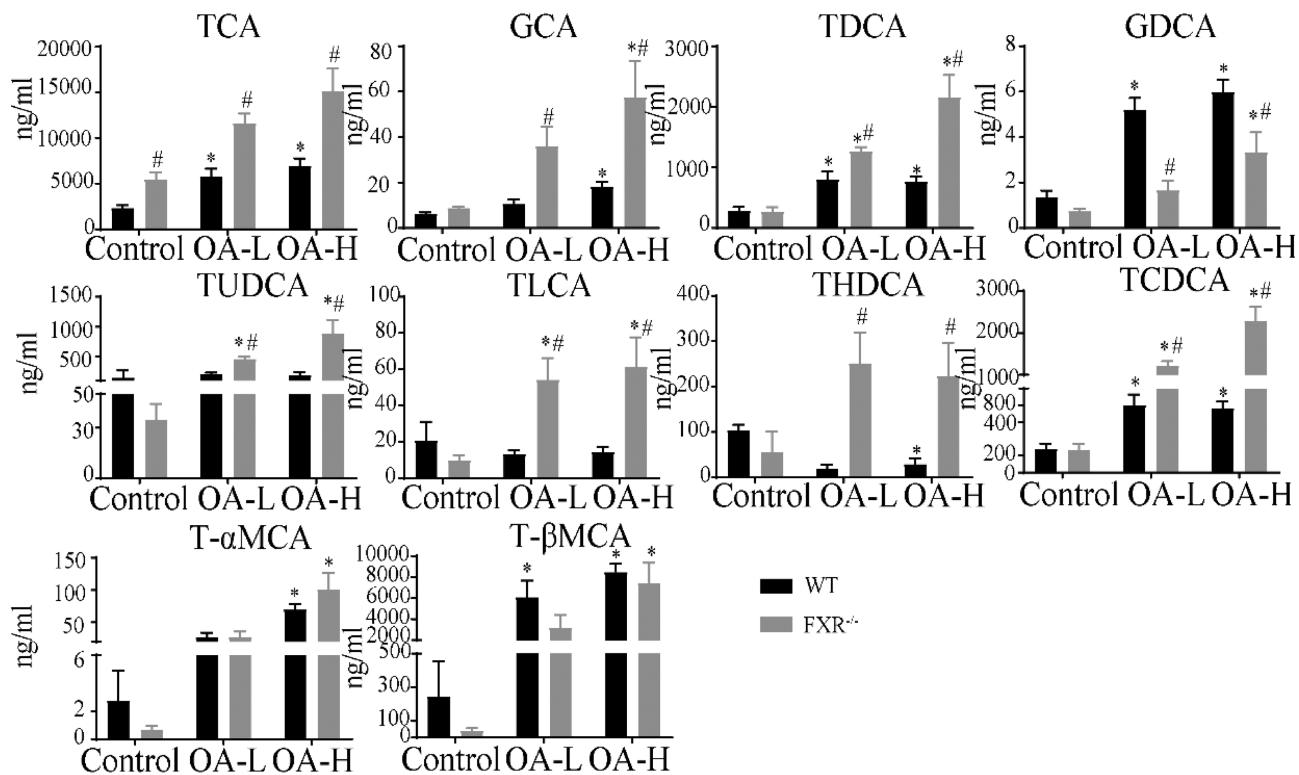
FIGURE 4 Levels of liver bile acids at 24 h after OA continuous administration for 4 days. The detection of the bile acids was performed as described in Section 2, and samples were collected at 24 h after the last dose (OA-L: oleanolic acid low dose group; OA-H: oleanolic acid high dose group). Data are presented as the mean ± SEM ($n = 3–5$). *$P < 0.05$, as compared with the control group without OA treatment; #$P < 0.05$, comparison between WT mice and FXR$^{-/-}$ mice under the same dose of OA treatment

cholestatic liver injury manifested as dynamic changes in the bile acids. We therefore analyzed the levels of liver bile acids at 3 h after the last dose following 4 days of continuous OA administration and found that T-αMCA level was significantly lower in the OA-H group in FXR$^{-/-}$ mice compared with that in the respective WT mice (Figure S1), indicating that knockdown of FXR$^{-/-}$ might reduce liver bile acids content in the early stage of OA administration. To further test this hypothesis, we measured the levels of liver bile acids after 3 h of a single administration of OA (Figure S2), and the results revealed that indeed GCA, TDCA, TUDCA, TLCA, THDCA, TCDCA, and T-α/βMCA levels were decreased in the OA-H group of FXR$^{-/-}$ mice compared with those in the WT OA-H mice. These results suggested that FXR$^{-/-}$ mice displayed a reduction in OA-induced cholestatic liver injury by reducing the liver bile acid levels in the early stage of OA administration.

When cholestatic liver injury occurs, the liver bile acid load may be lowered by excreting bile acids into the blood and biliary tract. We therefore investigated the level of bile acids in the serum and in the bile at 24 h after the last dose following 4 days of continuous OA administration. Serum bile acid concentrations may directly reflect the degree of liver damage. In the WT mice, the increases in TCA, GCA, TDCA, TUDCA, TLCA, THDCA, TCDCA, and T-α/βMCA levels were observed in the OA-H group compared with the control group. Similar results were observed in FXR$^{-/-}$ mice. Importantly, in the OA-H group, the content of TCA, GCA, TUDCA, TLCA, THDCA, TCDCA,

and T-α/βMCA in FXR$^{-/-}$ mice was lower than that in WT mice (Figure 5), which was in accordance with the serum TBA levels, suggesting that FXR$^{-/-}$ could alleviate cholestatic liver injury by reducing the serum bile acid levels.

Bile acid concentrations in the bile may directly reflect the efflux of bile acid in the liver. The levels of bile acids in the bile were determined at 24 h after the last dose following 4 days of continuous OA administration. As shown in Figure 6, in the WT mice, TCA, TDCA, THDCA, TUDCA, TCDCA, and T-α/βMCA in the bile were decreased in the OA-H group compared with the control group. In FXR$^{-/-}$ mice, the levels of all bile acids, with the exception of T-α/βMCA, were also decreased in the OA-H group compared with those in the control group. Moreover, TCA, TDCA, THDCA, TUDCA, and TCDCA were higher in FXR$^{-/-}$ mice than in WT mice when treated with high dose OA. All these results demonstrated that FXR$^{-/-}$ mice were resistant to OA-induced cholestatic liver injury by increasing bile acid efflux.

4.3 | mRNA expression levels of genes involved bile acids homeostasis are altered in FXR$^{-/-}$ mice compared with those in wild-type mice

FXR is known to regulate transporters and enzymes involved in bile acids homeostasis, and lower concentration bile acids were observed in FXR$^{-/-}$ mice in our experiment. Hence, we next investigated
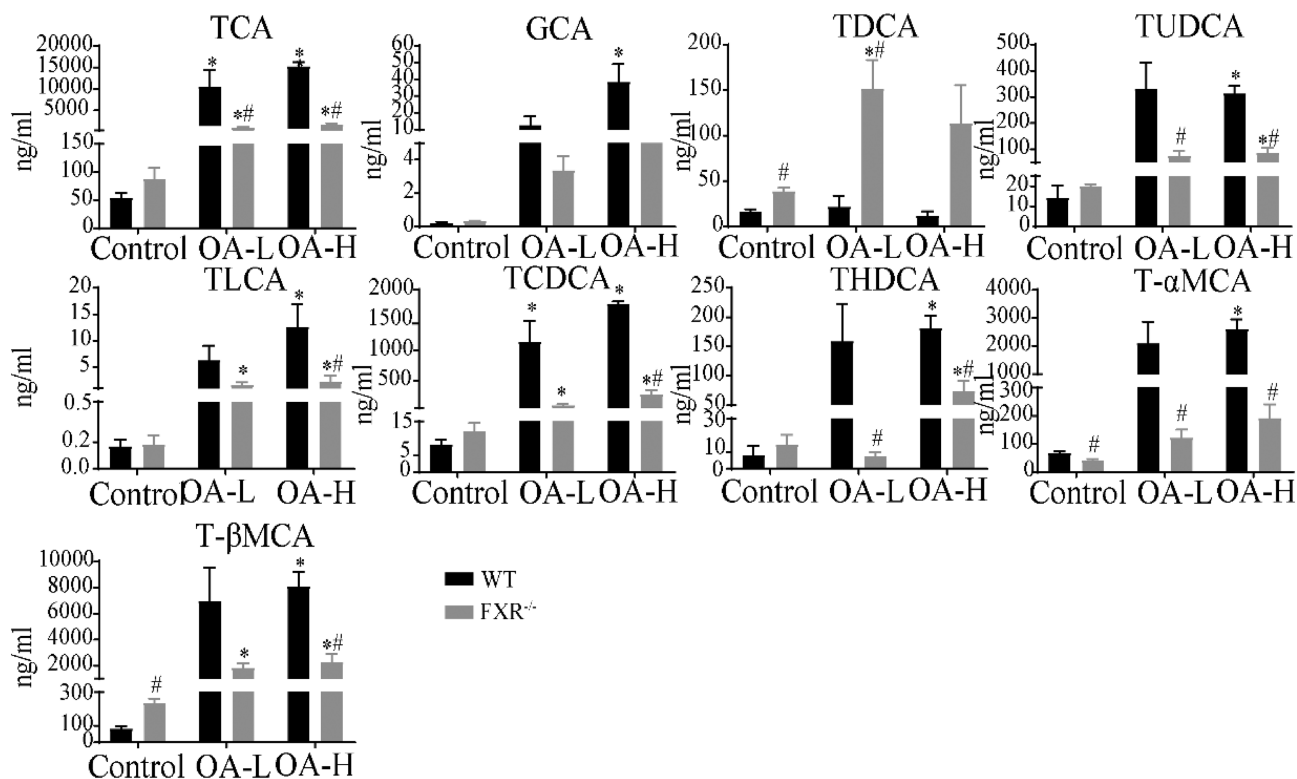
FIGURE 5 Levels of serum bile acids at 24 h after OA continuous administration for 4 days. The detection of the bile acids was performed as described in the section of materials and methods, and samples were collected at 24 h after the last dose (OA-L: oleanolic acid low dose group; OA-H: oleanolic acid high dose group); mean ± SEM ($n = 3–5$). *$P < 0.05$, as compared with the control group without OA treatment; #$P < 0.05$, comparison between WT mice and FXR$^{-/-}$ mice under the same dose of OA treatment
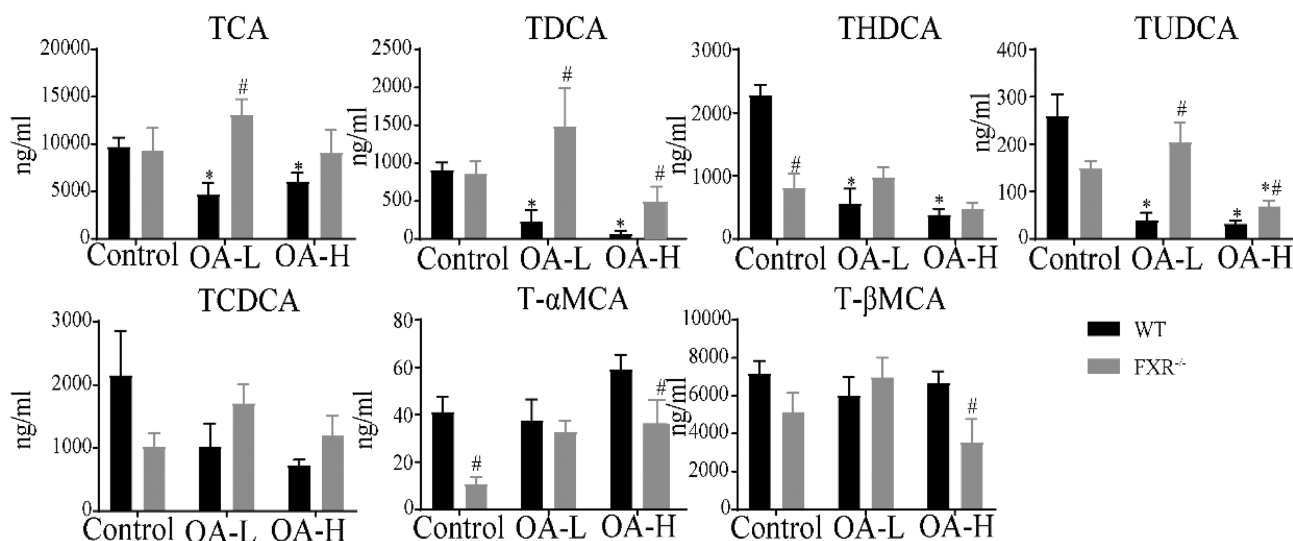
FIGURE 6 Levels of bile acids in the bile at 24 h after OA continuous administration for 4 days. The detection of the bile acids was performed as described in Section 2, and samples were collected at 24 h after the last dose (OA-L: oleanolic acid low dose group; OA-H: oleanolic acid high dose group). Data are presented as the mean ± SEM ($n = 3–5$). *$P < 0.05$, as compared with the control group without OA treatment; #$P < 0.05$, comparison between WT mice and FXR$^{-/-}$ mice under the same dose of OA treatment

mRNA expression levels in the liver of genes involved in regulation of bile acid homeostasis at 24 h after the last dose following 4 days of continuous OA administration. Following OA treatment, *Fxr* mRNA was dose-dependently suppressed in WT mice (Figure 7). Similarly, in WT mice, the bile acid efflux transporters (*Bsep*, *Mdr2*, and *Mrp2*) and uptake transporters (*Ntcp*, *Oatp1b2*) were also significantly
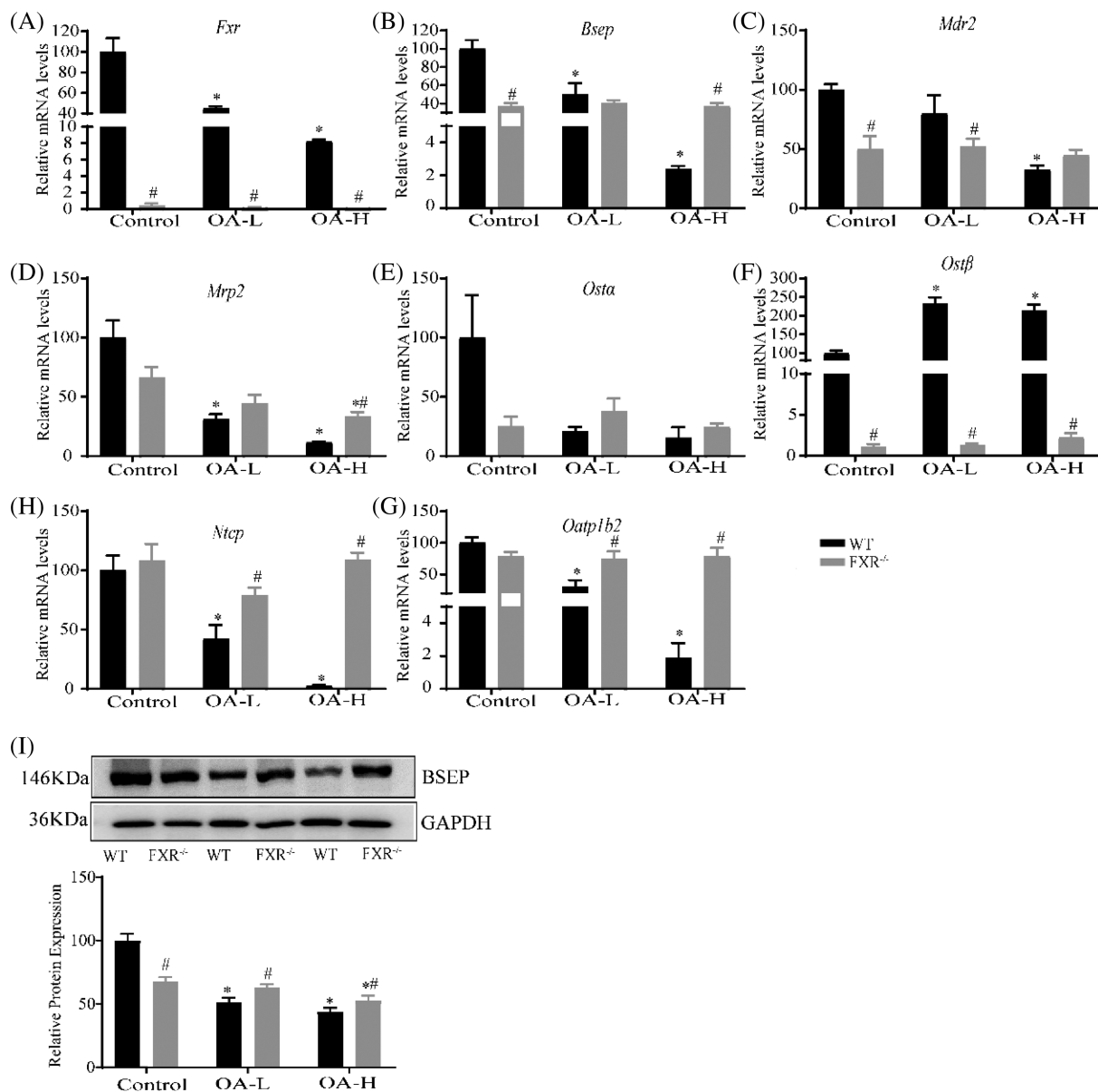
FIGURE 7 The mRNA and protein expression levels of liver bile acid transporters. Samples were collected at 24 h after the last dose following continuous OA continuous administration for 4 days (OA-L: oleanolic acid low dose group; OA-H: oleanolic acid high dose group). (A–G) Bile acid efflux transporters and uptake transporters. (I) Protein level of membrane protein BSEP in the liver. Data are presented at mean ± SEM (n = 5–8). *P < 0.05, as compared with the control group without OA treatment; #P < 0.05, comparison between WT mice and FXR$^{-/-}$ mice under the same dose of OA treatment

suppressed in the OA-H group compared with the control group (Figure 7), while the gene expression of the transporter $Ost\beta$ that is responsible for the efflux of bile acids back into the blood was increased. In addition, the expression of BSEP membrane protein in the liver was down-regulated after OA treatment as determined by Western blotting (Figure 7). On the contrary, there were no noticeable changes in the mRNA expression levels of these genes in FXR$^{-/-}$ mice between the control group and OA treated groups. Interestingly, in the OA-H group, the mRNA expression of $Bsep$, $Mdr2$, $Mrp2$, $Ntcp$, and $Oatp1b2$ was significantly higher in FXR$^{-/-}$ mice compared with WT mice, which was also observed for BSEP membrane protein

expression. These results indicated that increased mRNA expression of bile acid transporters might contribute to mild liver damage in FXR$^{-/-}$ mice relative to WT mice when treated with OA.

We next determined the mRNA expression levels of bile acid synthesis enzymes (Shp, $Cyp7a1$, $Cyp8b1$, $Cyp27a1$, and $Cyp7b1$) and bile acid conjugated enzymes ($Baat$ and $Bacs$) in the liver. As shown in Figure 8, in WT mice, the mRNA expression levels of Shp, $Cyp7a1$, $Cyp8b1$, $Cyp27a1$, $Cyp7b1$, Baat, and Bacs were suppressed in the OA-H group compared with the control group. In FXR$^{-/-}$ mice, the mRNA expression levels of these same genes were also suppressed in the OA-H group compared with the control group. However, the
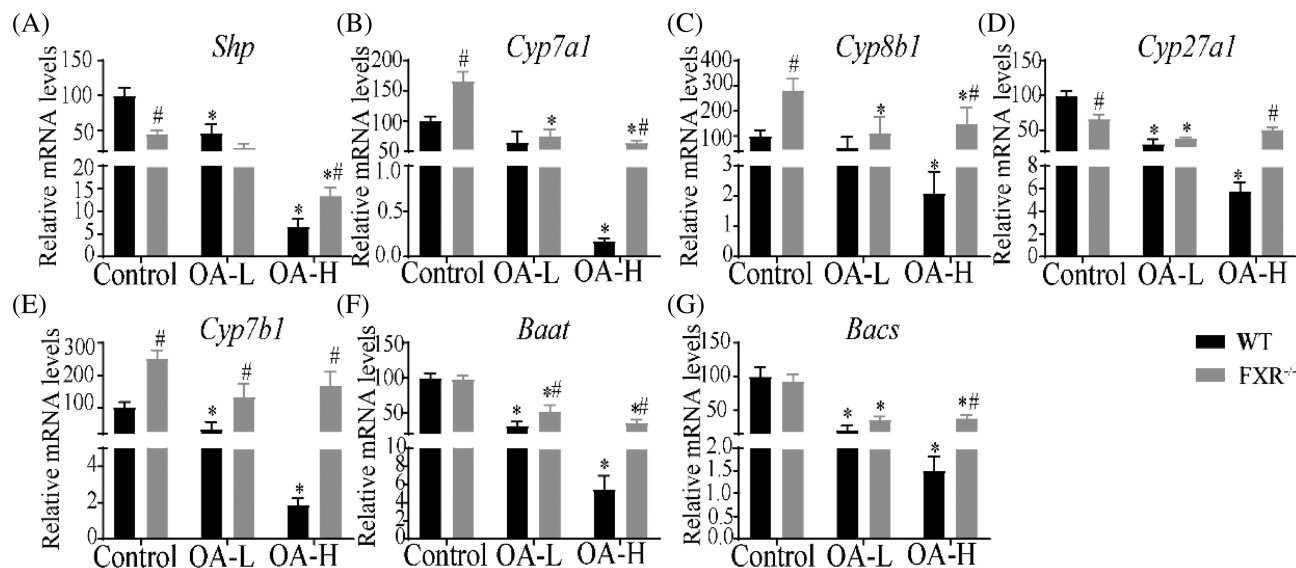
FIGURE 8 The mRNA expression levels of liver bile acid synthesis enzymes and conjugated enzymes after OA continuous administration for 4 days. Samples were collected at 24 h after the last dose (OA-L: oleanolic acid low dose group; OA-H: oleanolic acid high dose group). Data are presented as the mean ± SEM ($n = 5$–8). *$P < 0.05$, as compared with the control group without OA treatment; #$P < 0.05$, comparison between WT mice and FXR$^{-/-}$ mice under the same dose of OA treatment
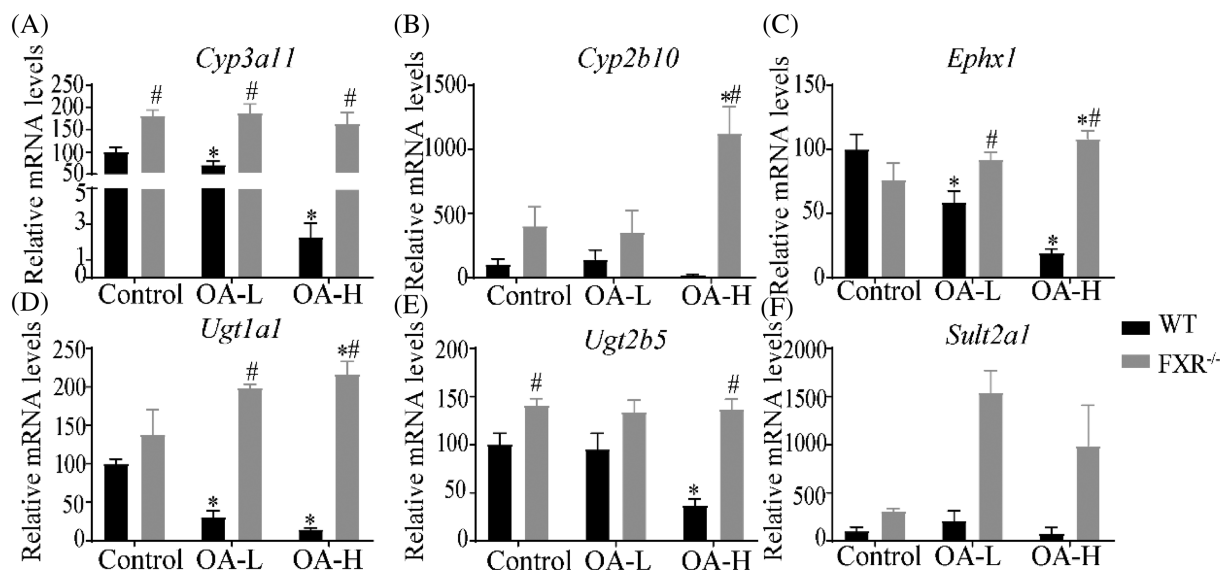
FIGURE 9 The mRNA expression levels of liver bile acid detoxifying enzymes after OA continuous administration for 4 days. Samples were collected at 24 h after the last dose (OA-L: oleanolic acid low dose group; OA-H: oleanolic acid high dose group). Data are presented as the mean ± SEM ($n = 5$–8). *$P < 0.05$, as compared with the control group without OA treatment; #$P < 0.05$, comparison between WT mice and FXR$^{-/-}$ mice under the same dose of OA treatment

mRNA expressions of these genes remained significantly higher in FXR$^{-/-}$ OA-H mice compared with WT OA-H mice, suggesting that an increase in the synthesis of bile acids might not be the only cause of OA-induced cholestatic liver injury.

To further explore the causes of less liver injury in FXR$^{-/-}$ mice, we analyzed the mRNA expression of the liver bile acids detoxifying enzymes *Cyp3a11*, *Cyp2b10*, *Ephx1*, *Ugt1a1*, *Ugt2b5*, and *Sult2a1* (Figure 9). We found that the mRNA expressions of *Cyp3a11*, *Ephx1*, *Ugt1a1*, and *Ugt2b5* were suppressed in WT OA-H mice compared

with the WT mice controls, while the mRNA expressions of *Cyp2b10*, *Ephx1*, and *Ugt1a1* were significantly increased in FXR$^{-/-}$ OA-H mice compared with the FXR$^{-/-}$ control. Obviously, the mRNA expression levels of the detoxifying enzymes *Cyp3a11*, *Cyp2b10*, *Ephx1*, *Ugt1a1*, and *Ugt2b5* were much higher in FXR$^{-/-}$ mice compared with WT mice in the OA-H treated group. Overall, these results indicated that FXR knockdown might reduce the OA-induced cholestatic liver injury by up-regulating the mRNA expression of liver bile acid detoxification enzymes.

5 | DISCUSSION

In the present study we demonstrated that cholestatic liver injury was observed 24 h after the final dose of a 4-day continuous administration of high dose OA. FXR$^{-/-}$ mice were protected from OA-induced cholestatic liver injury, which might be attributed to not only the increased mRNA expression of Bsep, Cyp3a11, Cyp2b10, Ephx1, Ugt1a1, Ugt2b5, Bacs, and Baat, but also to the decreased bile acid overload.

At present, ALP > 2 times ULN is used as the basis for determining the diagnostic criteria of cholestatic liver injury based on the "Practical Guidelines for the Diagnosis and Early Treatment of Drug-induced Liver Injury" (Tajiri & Shimizu, 2008). In the study of cholestatic liver injury, animal models often combine evidence of cholestasis, intrahepatic bile duct dilatation, hepatocyte feathery degeneration and other typical pathologies (Khamphaya et al., 2016). In the present study, we showed that the ALP was >2 times ULN in WT mice treated with OA-H for 4 days, along with hepatocyte necrosis and increased ALT, AST, and TBA levels. However, a significant lower ALP level (1.45 times the ULN) was observed in FXR$^{-/-}$ mice treated with OA-H. Histopathological examination of liver tissues also revealed less hepatocytes necrosis in FXR$^{-/-}$ mice treated with OA-H. Accordingly, our results clearly indicated that high dose OA induced cholestatic liver injury in WT mice, while liver damage in FXR$^{-/-}$ mice was reduced.

Bile acids are the main components of bile and are responsible for promoting the absorption of lipids and fat-soluble vitamins, which play an important role in maintaining cholesterol metabolism. Dysfunction in the formation, secretion, and excretion of bile acids may lead to the accumulation of a large amount of bile acids in the liver, which in turn leads to liver damage (Kong et al., 2013; Liu et al., 2019). It has been reported that the decrease in bile acid content in the serum and liver can be used as a prognostic indicator of cholestatic liver injury, while the increased bile acid content in the bile can reduce the liver toxicity induced by bile acid (Li et al., 2019; Wang et al., 2014, 2017, 2020). Our results were consistent with the observations in a study showing that the Xiaoyan Lidan Formula ameliorates ANIT-induced intrahepatic cholestatic liver injury in rats by reversing the increase of hepatic bile acids and decreasing serum bile acids levels induced by ANIT (Zhang et al., 2020). In this work, the elevated serum bile acids and increased bile acids in the bile were also observed in FXR$^{-/-}$ mice, which may in part explain why FXR$^{-/-}$ mice may have a reduction in the OA-induced cholestatic liver injury.

Unexpectedly, modest liver injury was observed in FXR$^{-/-}$ mice at 24 h after the last dose following treatment with OA for 4 days, but the levels of liver bile acids increased, which was inconsistent with findings from previous studies (Anakk et al., 2011; Kong et al., 2019). It has been reported that changes in bile acids are related to the duration of drug exposure, doses administered, and compensatory mechanisms involved in the process of cholestatic liver injury (Tian et al., 2017). To further understand changes in liver bile acids caused by OA in FXR$^{-/-}$ mice, a similar analysis was made for liver bile acids at 3 h after the last dose of 4-day OA administration. In this context, T-αMCA levels were decreased in FXR$^{-/-}$ mice compared with WT

mice after OA treatment. Thus, we postulated that FXR$^{-/-}$ mice exhibited reduced hepatotoxicity due to low content bile acids in the early stages of OA administration. This hypothesis was further supported by the measurement of liver bile acids at 3 h following a single administration of OA, which showed a significant reduction of TCA, GCA, TUDCA, TLCA, THDCA, TCDCA, and T-α/βMCA in FXR$^{-/-}$ mice compared with WT mice. These results implied that FXR$^{-/-}$ mice attenuated the OA-induced cholestatic hepatotoxicity by reducing the level of liver bile acid in the early stage, while the lower content of intrahepatic bile acids in the WT mice might be the self-protection function of WT mice after OA-induced cholestatic liver injury.

There are many enzymes and transporters that participate in bile acid homeostasis, and essentially, all are regulated by FXR (Schadt et al., 2016). Inhibition of FXR may upregulate the expression of bile acid synthases (Cyp7a1, Cyp8b1, Cyp27a1, and Cyp7b1) and reuptake transporters (Ntcp, Oatp), resulting in the accumulation of liver bile acids and inducing liver injury (Zhong et al., 2018). The mRNA expression of bile acid synthases and bile acid uptake transporters decreased in WT mice following OA-H treatment; however, a similar decrease in the gene expression of these bile acid synthases and bile acid uptake transporters was not observed in FXR$^{-/-}$ mice after OA-induced cholestatic liver injury. These results could in part explain why the intrahepatic bile acid content of FXR$^{-/-}$ mice was higher than that of WT mice at 24 h after the final dose of a 4-day continuous administration of high dose OA, suggesting that FXR$^{-/-}$ mice might reduce OA-induced liver damage through other ways, such as bile acid efflux. However, the regulation of these bile acid synthases and uptake transporters in the scenario of OA treatment and FXR knockdown warrants further investigation. Other studies have noted that inhibition of FXR downregulates the expression of the bile acid efflux transporters Bsep, Mdr2, and Mrp2, leading to the accumulation liver bile acids and subsequent liver damage (Guo et al., 2016). Given that BSEP is the main bile acid efflux transporter and is responsible for transporting conjugated bile acids (Song et al., 2015), we evaluated the expression of BSEP protein. The expression of Bsep mRNA and BSEP protein was markedly higher in FXR$^{-/-}$ mice than in WT mice when treated with OA, suggesting that knockdown of FXR promoted liver bile acids efflux, and thus, reduced the toxicity caused by OA (Figure 10). Our findings demonstrated that the disruption of Bsep-mediated efflux was the dominant factor involved in OA-induced cholestatic liver injury. Previous studies (Sayin et al., 2013; Song et al., 2015) have shown that the expression of Bsep was suppressed in FXR gene knockout mice. It is worthy to note that in the present study, we observed a similar downregulation of Bsep in the liver of FXR$^{-/-}$ mice compared with the WT control (Figure 7). However, our results showed that the expression of Bsep mRNA and BSEP protein was significantly higher in the liver of FXR$^{-/-}$ mice compared with WT mice when treated with OA. The increase in Bsep expression does not appear to be solely mediated by FXR, other mechanisms, such as Nrf2, glucocorticoid receptor, and other nuclear (hormone) receptors in cholestasis (Martin et al., 2010; Weerachayaphorn et al., 2010), might also be involved, which need to be further
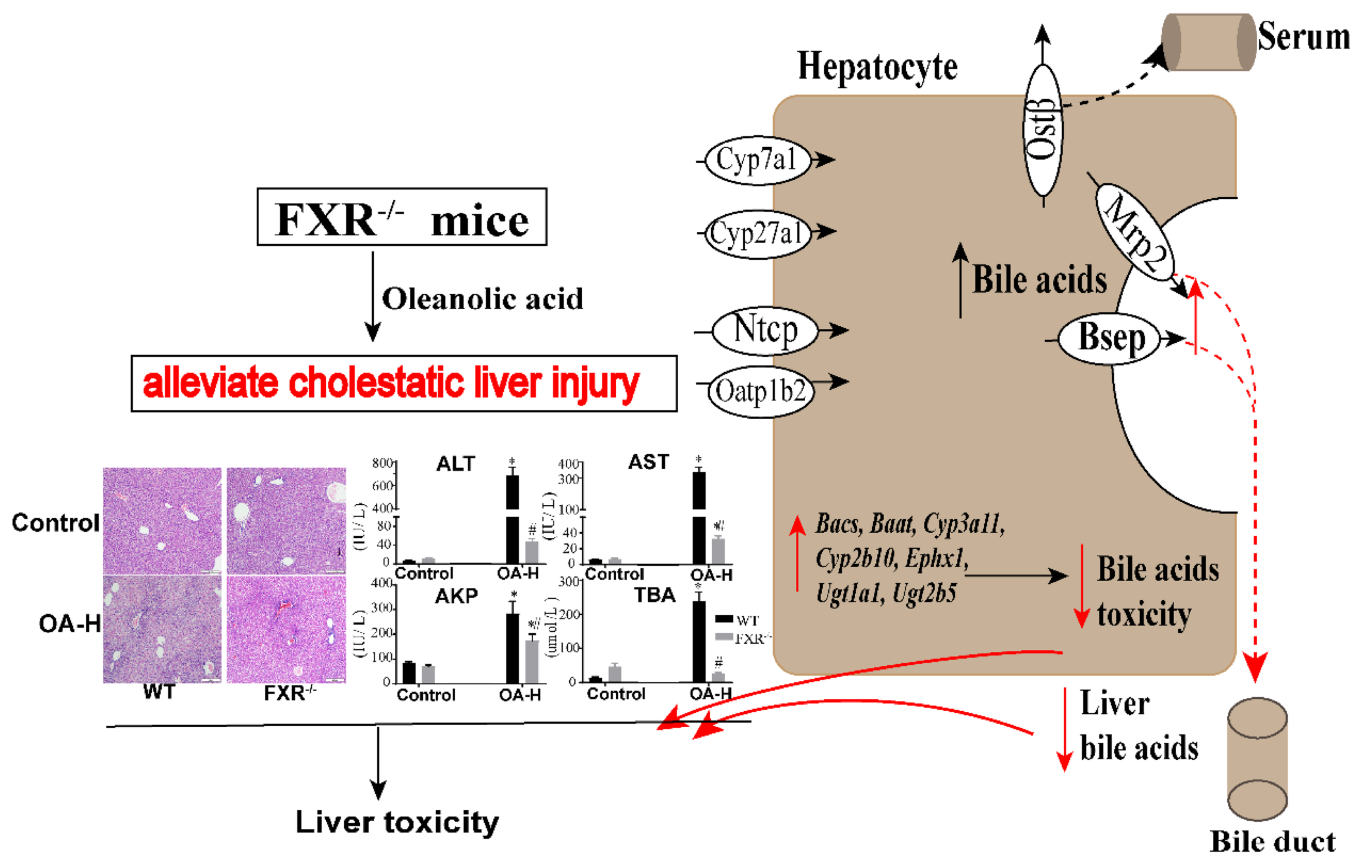
FIGURE 10 A proposed scheme of mechanism by which knockdown of FXR alleviates OA-induced cholestatic liver injury

explored. It is generally believed that the increased expression of bile acid detoxifying enzymes and conjugated enzymes is also related to the reduction of cholestatic liver injury. Compared with WT mice after OA treatment, the expressions of conjugating enzymes *Baat* and *Bacs* in FXR$^{-/-}$ mice were significantly higher. The increase in the expression of these conjugating enzymes may enhance the conjugation of bile acids and thus reduce their toxicity. In addition, we observed significantly higher expressions of bile acid detoxification enzymes *Cyp3a11*, *Cyp2b10*, *Ugt1a1*, *Ugt2b5*, and *Ephx1* in the FXR$^{-/-}$ mice compared with the WT mice when treated with OA. In the cases of *Cyp2b10*, *Ugt1a1*, and *Ephx1*, an induction of gene expression caused by OA treatment was also present in the FXR$^{-/-}$ mice. The increased expression of these detoxification enzymes may be involved in the polyhydroxylation, sulfation, or glycosylation of toxic bile acids, converting them into more hydrophilic substances for excretion (Figure 10), thereby reducing bile acid toxicity (Cho et al., 2010). Although the exact mechanism has yet to be defined, these adaptive changes in the FXR-null mice may play an important role in alleviating OA-induced cholestatic liver injury.

6 | CONCLUSION

In this study, we demonstrated that OA-induced cholestatic liver injury in mice was significantly reduced when FXR was knocked out.

This phenomenon may be mediated through the modulation of the expressions of genes involved in the export and synthesis of bile acids, leading to a decrease in the accumulation of bile acids both in the liver and serum, as well as the upregulation of bile acids detoxification enzymes.

CONFLICT OF INTEREST
The authors declare that they have no conflict of interest.

AUTHOR CONTRIBUTIONS
Yuanfu Lu, Shaoyu Zhou, Feng Hong, and Yan Hu designed the experiments. Hong Feng performed the main experiments and wrote the paper. Yuanfu Lu and Shaoyu Zhou revised the paper. Yan Hu participated in part of the experiments. All authors reviewed and approved the final version of the manuscript.

ORCID

Hong Feng https://orcid.org/0000-0002-9176-5265
Yuanfu Lu https://orcid.org/0000-0002-0698-1597

REFERENCES

Anakk, S., Watanabe, M., Ochsner, S. A., McKenna, N., Finegold, M. J., & Moore, D. D. (2011). Combined deletion of FXR and SHP in mice induces CYP17a1 and results in juvenile onset cholestasis. *The Journal of Clinical Investigation*, *121*(1), 86–95. https://doi.org/10.1172/JCI42846

Cariello, M., Piccinin, E., Garcia-Irigoyen, O., Sabbà, C., & Moschetta, A. (2018). Nuclear receptor FXR, bile acids and liver damage: Introducing the progressive familial intrahepatic cholestasis with FXR mutations. *Biochimica et biophysica acta. Molecular Basis of Disease*, *1864*(4 Pt B), 1308–1318. https://doi.org/10.1016/j.bbadis.2017.09.019

Cho, J. Y., Matsubara, T., Kang, D. W., Ahn, S. H., Krausz, K. W., Idle, J. R., Luecke, H., & Gonzalez, F. J. (2010). Urinary metabolomics in Fxr-null mice reveals activated adaptive metabolic pathways upon bile acid challenge. *Journal of Lipid Research*, *51*(5), 1063–1074. https://doi.org/10.1194/jlr.M002923

Feng, H., & Lu, Y. F. (2020). Role of Farnesoid X receptor (FXR) in drug-induced cholestatic liver injury. *Journal of Zunyi Medical University*, *43*(04), 116–124. https://doi.org/10.14169/j.cnki.zunyixuebao.2020.0097

Feng, H., Wu, Y. Q., Xu, Y. S., Wang, K. X., Qin, X. M., & Lu, Y. F. (2020). LC-MS-based metabolomic study of oleanolic acid-induced hepatotoxicity in mice. *Frontiers in Pharmacology*, *11*, 747. https://doi.org/10.3389/fphar.2020.00747

Guo, H. L., Hassan, H. M., Zhang, Y., Dong, S. Z., Ding, P. P., Wang, T., Sun, L. X., Zhang, L. Y., & Jiang, Z. Z. (2016). Pyrazinamide induced rat cholestatic liver injury through inhibition of FXR regulatory effect on bile acid synthesis and transport. *Toxicological Sciences*, *152*(2), 417–428. https://doi.org/10.1093/toxsci/kfw098

Hoofnagle, J. H., & Björnsson, E. S. (2019). Drug-induced liver injury-types and phenotypes. *The New England Journal of Medicine*, *381*(3), 264–273. https://doi.org/10.1056/NEJMra1816149

Huang, S. (2019). Effects of alkaloids from *Dendrobium nobile* Lindl. on lipid homeostasis in mice fed by high-fat diet via bile acids metabolism. Zunyi Medical University Graduate Thesis, 21–22

Huang, S., Wu, Q., Liu, H., Ling, H., He, Y. Q., Wang, C. H., Wang, Z., Lu, Y., & Lu, Y. F. (2019). Alkaloids of *Dendrobium nobile* Lindl. altered hepatic lipid homeostasis via regulation of bile acids. *Journal of Ethnopharmacology*, *241*, 111976. https://doi.org/10.1016/j.jep.2019.111976

Kawashita, E., Ishihara, K., Nomoto, M., Taniguchi, M., & Akiba, S. (2019). A comparative analysis of hepatic pathological phenotypes in C57BL/6J and C57BL/6N mouse strains in non-alcoholic steatohepatitis models. *Scientific Reports*, *15*(9), e0232069. https://doi.org/10.1371/journal.pone.0232069

Khamphaya, T., Chansela, P., Piyachaturawat, P., Suksamrarn, A., Nathanson, M. H., & Weerachayaphorn, J. (2016). Effects of andrographolide on intrahepatic cholestasis induced by alpha-naphthylisothiocyanate in rats. *European Journal of Pharmacology*, *789*, 254–264. https://doi.org/10.1016/j.ejphar.2016.07.032

Kong, B., Zhang, M., Huang, M. X., Rizzolo, D., Armstrong, L. E., Schumacher, J. D., & Grace, L. G. (2019). FXR deficiency alters bile acid pool composition and exacerbates chronic alcohol induced liver injury. *Digestive and Liver Disease*, *51*(4), 570–576. https://doi.org/10.1016/j.dld.2018.12.026

Kong, D., Zhang, F., Wei, D. H., Zhu, X. J., Zhang, X. P., Chen, L., & Zheng, S. Z. (2013). Paeonol inhibits hepatic fibrogenesis via disrupting NF-κB pathway in activated stellate cells: In vivo and in vitro studies. *Journal of Gastroenterology and Hepatology*, *28*(7), 1223–1233. https://doi.org/10.1111/jgh.12147

Li, T., & Apte, U. (2015). Bile acid metabolism and signaling in cholestasis, inflammation, and cancer. *Advances in Pharmacology*, *74*, 263–302. https://doi.org/10.1016/bs.apha.2015.04.003

Li, T., & Chiang, J. Y. (2013). Nuclear receptors in bile acid metabolism. *Drug Metabolism Reviews*, *45*(1), 145–155. https://doi.org/10.3109/03602532.2012.740048

Li, W. K., Wang, G. F., Wang, T. M., Li, Y. Y., Li, Y., Lu, X. Y., Wang, Y. H., Zhang, H., Liu, P., Wu, J. S., & Ma, Y. M. (2019). Protective effect of herbal medicine Huangqi decoction against chronic cholestatic liver injury by inhibiting bile acid-stimulated inflammation in DDC-induced mice. *Phytomedicine*, *62*, 152948. https://doi.org/10.1016/j.phymed.2019.152948

Liu, J., Lu, Y. F., Wu, Q., Xu, S. F., Shi, F. G., & Klaassen, C. D. (2018). Oleanolic acid reprograms the liver to protect against hepatotoxicants, but is hepatotoxic at high doses. *Liver International*, *39*(3), 427–439. https://doi.org/10.1111/liv.13940

Liu, J., Lu, Y. F., Zhang, Y. C., Wu, K. C., Fan, F., & Klaassen, C. D. (2013). Oleanolic acid alters bile acid metabolism and produces cholestatic liver injury in mice. *Toxicology and Applied Pharmacology*, *272*(3), 816–835. https://doi.org/10.1016/j.taap.2013.08.003

Liu, R., Li, X., Huang, N., Fan, M., & Sun, R. (2020). Toxicity of traditional Chinese medicine herbal and mineral products. *Advances in Pharmacology*, *87*, 301–346. https://doi.org/10.1016/bs.apha.2019.08.001

Liu, Y. H., Chen, K. F., Li, F. Y., Gu, Z. L., Liu, Q., He, L. Q., Shao, T., Song, Q., Zhu, F., Zhang, L., Jiang, M., Zhou, Y., Barve, S., Zhang, X., McClain, C. J., & Feng, W. K. (2019). Probiotic lactobacillus rhamnosus GG prevents liver fibrosis through inhibiting hepatic bile acid synthesis and enhancing bile acid excretion in mice. *Hepatology*, *71*(6), 2050–2066. https://doi.org/10.1002/hep.30975

Lu, Y. F., Wan, X. L., Xu, Y. S., & Liu, J. (2013). Repeated oral administration of oleanolic acid produces cholestatic liver injury in mice. *Molecules*, *18*(3), 3060–3071. https://doi.org/10.3390/molecules18033060

Lu, Y. L., Du, Y. M., Qin, L., Ma, F. F., Ling, L., Yang, T., Lu, A. J., Wu, D., Zhou, X. M., & He, Y. Q. (2018). Hypolipemic mechanism of saponins from Gynostemma Pentaphylla based on analysis of bile acids. *Natural Product Research and Development*, *30*, 1143–1148. https://doi.org/10.16333/j.1001-6880.2018.7.008

Lu, Y. L., Du, Y. M., Qin, L., Wu, D., Wang, W., Ling, L., Ma, F., Ling, H., Yang, L., Wang, C., Wang, Z., Zhou, X., & He, Y. Q. (2018). Gypenosides altered hepatic bile acids homeostasis in mice treated with high fat diet. *Evidence-Based Complementary and Alternative Medicine*, *2018*, 8098059. https://doi.org/10.1155/2018/8098059

Martin, W., Gernot, Z., & Michael, T. (2010). Nuclear receptor regulation of the adaptive response of bile acid transporters in cholestasis. *Seminars in Liver Disease*, *30*(2), 160–177. https://doi.org/10.1055/s-0030-1253225

Oh, S. J., Cho, J. H., & Son, C. G. (2015). Systematic review of the incidence of herbal drug-induced liver injury in Korea. *Journal of Ethnopharmacology*, *159*, 253–258. https://doi.org/10.1016/j.jep.2014.11.027

Oz, H. S., McClain, C. J., Nagasawa, H. T., Ray, M. B., de Villiers, W. J., & Chen, T. S. (2003). Diverse antioxidants protect against acetaminophen hepatotoxicity. *Journal of Biochemical and Molecular Toxicology*, *18*, 363–368. https://doi.org/10.1002/jbt.20042

Sayin, S. I., Wahlström, A., Felin, J., Jäntti, S., Marschall, H. U., Bamberg, K., Angelin, B., Hyötyläinen, T., Orešič, M., & Bäckhed, F. (2013). Gut microbiota regulates bile acid metabolism by reducing the levels of tauro-beta-muricholic acid, a naturally occurring FXR antagonist. *Cell Metabolism*, *17*(2), 225–235. https://doi.org/10.1016/j.cmet.2013.01.003

Schadt, H. S., Wolf, A., Pognan, F., Chibout, S. D., Merz, M., & Kullak-Ublick, G. A. (2016). Bile acids in drug induced liver injury: Key players and surrogate markers. *Clinics and Research in Hepatology and Gastroenterology*, *40*(3), 257–266. https://doi.org/10.1016/j.clinre.2015.12.017

Shi, F. G., Pan, H., Cui, B. D., Li, Y., Huang, L. Y., & Lu, Y. F. (2019). Dictamnine-induced hepatotoxicity in mice: The role of metabolic activation of furan. *Toxicology and Applied Pharmacology*, *364*, 68–76. https://doi.org/10.1016/j.taap.2018.12.012

Shin, D. J., & Wang, L. (2019). Bile acid-activated receptors: A review on FXR and other nuclear receptors. *Handbook of Experimental Pharmacology*, *256*, 51–72. https://doi.org/10.1007/164_2019_236

Song, P. Z., Cheryl, E. R., Julia, Y. C., & Klaassen, C. D. (2015). Individual bile acids have differential effects on bile acid signaling in mice. *Toxicology and Applied Pharmacology*, *283*(1), 57–64. https://doi.org/10.1016/j.taap.2014.12.005

Stedman, C., Liddle, C., Coulter, S., Sonoda, J., Alvarez, J. G., Evans, R. M., & Downes, M. (2006). Benefit of farnesoid X receptor inhibition in obstructive cholestasis. *Proceedings of the National Academy of Sciences of the United States of America*, *103*(30), 11323–11328. https://doi.org/10.1073/pnas.0604772103

Tajiri, K., & Shimizu, Y. (2008). Practical guidelines for diagnosis and early management of drug-induced liver injury. *World Journal of Gastroenterology*, *14*(44), 6774–6785. https://doi.org/10.3748/wjg.14.6774

Tian, J., Zhu, J., Yi, Y., Li, C. Y., Zhang, Y. S., Zhao, Y., Pan, C., Xiang, S., Li, X., Li, G., Newman, J. W., Feng, X., Liu, J., Han, J., Wang, L., Gao, Y., La Frano, M. R., & Liang, A. (2017). Dose-related liver injury of Geniposide associated with the alteration in bile acid synthesis and transportation. *Scientific Reports*, *7*(1), 8938. https://doi.org/10.1038/s41598-017-09131-2

Trauner, M., Gulamhusein, A., Hameed, B., Caldwell, S., Shiffman, M. L., Landis, C., Eksteen, B., Agarwal, K., Muir, A., Rushbrook, S., Lu, X., Xu, J., Chuang, J.-C., Billin, A. N., Li, G., Chung, C., Subramanian, G. M., Myers, R. P., Bowlus, C. L., & Kowdley, K. V. (2019). The nonsteroidal farnesoid X receptor agonist Cilofexor (GS-9674) improves markers of cholestasis and liver injury in patients with primary sclerosing cholangitis. *Hepatology*, *70*(3), 788–801. https://doi.org/10.1002/hep.30509

Wang, G. F., Li, Y. Y., Shi, R., Wang, T. M., Li, Y. F., Li, W. K., Zheng, M., Fan, F. B., Zou, J., Zan, B., Wu, J. S., & Ma, Y. M. (2020). Yinchenzhufu decoction protects against alpha-naphthylisothiocyanate-induced acute cholestatic liver injury in mice by ameliorating disordered bile acid homeostasis and inhibiting inflammatory responses. *Journal of Ethnopharmacology*, *254*, 112672. https://doi.org/10.1016/j.jep.2020.112672

Wang, H., Fang, Z. Z., Meng, R., Cao, Y. F., Tanaka, N., Krausz, K. W., & Gonzalez, F. J. (2017). Glycyrrhizin and glycyrrhetinic acid inhibits alpha-naphthyl isothiocyanate-induced liver injury and bile acid cycle disruption. *Toxicology*, *386*, 133–142. https://doi.org/10.1016/j.tox.2017.05.012

Wang, T., Zhou, Z. X., Sun, L. X., Li, X., Xu, Z. M., Chen, M., Zhao, G. L., Jiang, Z. Z., & Zhang, L. Y. (2014). Resveratrol effectively attenuates α-naphthyl-isothiocyanate-induced acute cholestasis and liver injury through choleretic and anti-inflammatory mechanisms. *Acta Pharmacologica Sinica*, *35*(12), 1527–1536. https://doi.org/10.1038/aps.2014.119

Weerachayaphorn, J., Cai, S. Y., Soroka, C. J., & Boyer, J. L. (2010). Nuclear factor erythroid 2-related factor 2 is a positive regulator of human bile salt export pump expression. *Hepatology*, *50*(5), 1588–1596. https://doi.org/10.1002/hep.23151

Wei, J., Xie, G. X., & Wei, P. (2018). Bile acid-microbiota cross-talk in gastrointestinal inflammation and carcinogenesis. *Nature Reviews. Gastroenterology & Hepatology*, *15*, 111–128. https://doi.org/10.1038/nrgastro.2017.119

Yang, T. T., Mei, H. F., Xu, D. Q., Zhou, W., Zhu, X. Y., Sun, L. X., Huang, X., Wang, X., Shu, T., Liu, J., Ding, J., Hassan, H. M., Zhang, L., & Jiang, Z. Z. (2017). Early indications of ANIT-induced cholestatic liver injury: Alteration of hepatocyte polarization and bile acid homeostasis. *Food and Chemical Toxicology*, *110*, 1–12. https://doi.org/10.1016/j.fct.2017.09.051

Yuan, Z. Q., & Li, K. W. (2016). Role of farnesoid X receptor in cholestasis. *Journal of Digestive Diseases*, *17*(8), 501–509. https://doi.org/10.1111/1751-2980.12378

Zhang, R. J., Huang, T., Zhang, Q. Y., Yao, Y. F., Liu, C. H., Lin, C. Z., & Zhu, C. C. (2020). Xiaoyan lidan formula ameliorates α-naphthylisothiocyanate-induced intrahepatic cholestatic liver injury in rats as revealed by non-targeted and targeted metabolomics. *Journal of Pharmaceutical and Biomedical Analysis*, *179*, 112966. https://doi.org/10.1016/j.jpba.2019.112966

Zhong, D. D., Xie, Z. W., Huang, B. Y., Zhu, S., Wang, G. Q., Zhou, H., Lin, S., Lin, Z., & Yang, B. X. (2018). Ganoderma lucidum polysaccharide peptide alleviates hepatosteatosis via modulating bile acid metabolism dependent on FXR-SHP/FGF. *Cellular Physiology and Biochemistry*, *49*(3), 1204–1220. https://doi.org/10.1159/000493297

SUPPORTING INFORMATION

Additional supporting information may be found in the online version of the article at the publisher's website.